Simulations of ITB *H*-Mode Tokamak Plasmas with Predictive Toroidal Velocity Model

Boonyarit Chatthong[1], Thawatchai Onjun[1*], Wisit Singhsomroje[2], Nopporn Poolyarat[3], Sujin Suwanna[1], and Roppon Picha[4]

[1] School of Manufacturing Systems and Mechanical Engineering, Sirindhorn International Institute of Technology, Thammasat University, Pathumthani, Thailand, 12121
[2] Department of Physics, Faculty of Science, Mahidol University, Bangkok, Thailand, 10400
[3] Department of Physics, Thammasat University, Pathumthani, Thailand, 12121
[4] Thailand Institute of Nuclear Technology, Bangkok, Thailand, 10900
*Corresponding Author: thawatchai@siit.tu.ac.th

Abstract

A model for predicting toroidal velocity in *H*-mode tokamak plasma after neutral beam heating is turned on is implemented in an integrated predictive modelling code BALDUR in order to self-consistently simulate the time-evolution of plasma current, temperature, and density profiles in tokamaks. In this model, the toroidal velocity is developed according to a theory of electromagnetism in which the toroidal velocity can be obtained from a current density flow in toroidal direction. The core transport model used in these simulations is a combination of a neoclassical transport model called NCLASS, and an anomalous transport model, semi-empirical Mixed Bohm/gyro-Bohm (Mixed B/gB) that includes ITB effects. The boundary condition of the plasma is assumed to be at the top of the pedestal. The pedestal temperature is calculated using a theory-based pedestal model which is based on a combination of magnetic and flow shear stabilization pedestal width scaling and an infinite-n ballooning pressure gradient model. Time evolution of plasma temperature and density profiles of 10 JET optimized shear discharges is compared among direct experimental measurements, simulated results using toroidal velocity model and simulation results using experimental toroidal velocity data. Qualitatively, ITB formations are identified and investigated. Quantitatively, statistical analysis including root mean square errors (RMSE) and offsets are used for comparison. It is found that the averaged RMSE and offset among these discharges are respectively 28.13% and -0.19 for ion temperature, 31.78% and -0.24 for electron temperature, and 15.00% and -0.07 for electron density.

***Keywords**:* Plasmas, Tokamak, Internal Transport Barrier, Toroidal Velocity, BALDUR.

1. Introduction

To produce significant fusion reactions inside a tokamak reactor, the plasma must reach certain conditions namely high plasma temperature, density, and long energy confinement time. Burning plasma experiments such as the ITER (International Thermonuclear Experimental Reactor) project [1] are designed to operate in the high confinement mode (*H*-mode) because in this regime, the H-mode plasmas generally provide high temperature and sufficient energy confinement time. It is known that the improved performance of *H*-mode results mainly from the formation of an edge transport barrier (ETB) [2], called the pedestal. The performance of *H*-mode plasmas can be further improved by the formation of an internal transport barrier (ITB) [3] in the core region. It is generally accepted that ω_{ExB} flow shear plays a crucial role in the formation of ITBs. Theoretically, the calculation of ω_{ExB} requires the information of toroidal. Consequently, it is important to develop a model for predicting toroidal velocity in order to predict the ITB formation in *H*-mode plasmas.

The development of the ω_{ExB} flow shear concept to describe the formation of ITBs in magnetic confinement devices is one of the breakthroughs in fusion plasma research [4]. It is found that the reduction of transport in the plasmas is associated with shear effects, in particular the velocity shear and magnetic shear [4]. Toroidal velocity is one of the terms used in calculation of ω_{ExB} flow shear. There have been studies of momentum and velocity transport in the poloidal direction but not much has been done in the toroidal direction [5-8]. In general, one can expect the form of toroidal velocity in terms of plasma parameters such as plasma density, plasma current or torque. The exact calculation of toroidal velocity is complicated since it requires much detailed information. In Ref. [9], a simple empirical base model is developed in which the toroidal velocity is assumed to be directly proportional to local ion temperature. The model has an advantage that it is straightforward and can be used in plasmas simulations simply. However, a theoretical base model should be developed as a substitution in order to make a better prediction. In this work, a theoretically derived model for predicting toroidal velocity is proposed by assuming that the velocity represents the flow of current density for ion particles in toroidal rotation.

In this work, the proposed toroidal velocity model is implemented in the 1.5D BALDUR integrated predictive modeling code to self-consistently simulate the time evolution of plasma current, density and temperature profiles for ITB plasmas. In all simulations, a semi-empirical mixed B/gB core transport model which can include ITB effect is used to compute anomalous transport. The formation of ITB in this model is caused by a suppression of anomalous transport due to ω_{ExB} flow shear and magnetic shear *s* [10]. The boundary conditions are expressed in terms of a pedestal model developed in Ref. [11]. In the pedestal model, the pedestal temperature was predicted using the estimation of pedestal width based on magnetic and flow shear stabilization and pedestal pressure gradient based on ballooning mode instability. In BALDUR, the value of ω_{ExB} can be calculated from the information of radial electric field, toroidal velocity (v_{tor}), and poloidal velocity. The code can calculate the electric field and the poloidal information can be obtained from NCLASS model. This paper focuses on the development of a theoretical-based model for predicting toroidal velocity using information of a local current density flow in toroidal direction at a given time. The model is tested by carrying out simulations of 10 JET optimized shear discharges obtained from the International Profile Database.

This paper is organized as follows: an introduction to BALDUR is given in section 2, along with the toroidal velocity model, the mixed B/gB model with ITB effects included and the ETB pedestal models; the simulations results and discussion are presented in section 3; and the summary is presented in section 4.

2. The 1.5D BALDUR code

This section introduces theories and models used in the calculation of plasma profiles, the BALDUR predictive modeling code is also introduced here. BALDUR integrated predictive modeling code [12] is a time-dependent one and a half dimensional transport modelling code which is used to compute many physical quantities in tokamaks. The code computes the plasma profiles such as time-evolution of electron density, electron and ion temperatures as in this paper. It can also be used to compute other physical quantities like impurity and hydrogen densities, magnetic q and other gas densities [13].

BALDUR code self-consistently computes these profiles by mixing many physical processes together in form of modules including transport, plasma heating, particle flux, boundary conditions, and sawtooth oscillations modules. It was found that BALDUR code can yield the simulation results that are in agreement with experimental data. For example, in Refs. [14, 15], the BALDUR simulations with either MMM95 transport model or Mixed B/gB transport model yielded the temperature profile agreement of about 10% relative Root Mean Square (RMS) deviation for both L-mode and H-mode plasmas.

2.1 The toroidal velocity model

In this work, a theoretical approach for developing toroidal velocity (v_{tor}) model is used. It is assumed that the toroidal velocity can be viewed as a current density flow of positive ions in toroidal direction as follows:

$$v_{tor} = \frac{J_{tor}}{en_i Z_{eff}}, \qquad (1)$$

where J_{tor} is the current density in toroidal direction, n_i is ion density, and Z_{eff} is effective charge of ion species.

Generally, the toroidal flow of charged particles is driven by two main sources, the induced electric field from a central transformer core and the torque generated by external heating like NBI, ICRH and RF heating. Even though the particles collide and bounce off one another, they generally drift in the same direction by these driven forces. Tokamak plasma is composed of electrons and many species of ions. In general, one can expect each species to obtain different velocity from the driving energy. In this work, it is assumed that all ions retain the same velocity. Note that the effect from electron is neglected here because the main heating schemes used here are NBI and ICRH which mainly affect ions. Therefore, it is expected that ion particles receive much more kinetic energy than electrons do. Fig. 1 illustrates radial profile of experimental toroidal velocity of JET discharges 40542 and 40847 at their respective diagnostic time. The plots also include toroidal current density data from simulations. They appear to show similar profile shape like high value near the center, low value near the edge and relative flat profile at the regions close to both boundaries.

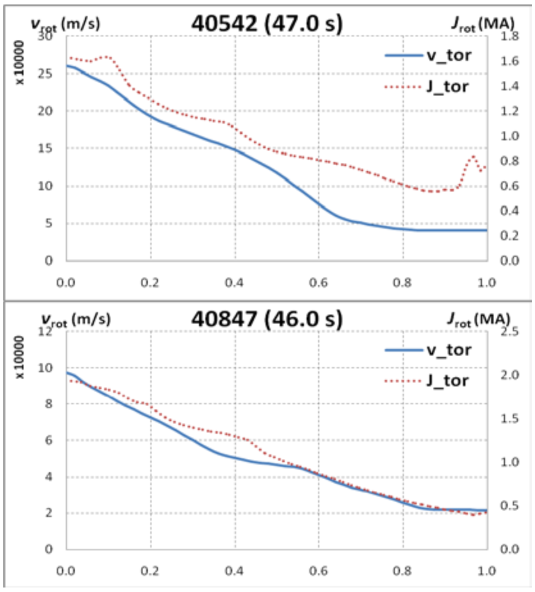

Fig. 1 Profile plots of toroidal velocity (left y-axis) together with toroidal current density (right y-axis) as a function of *r/a* (normalized minor radius) of JET 40542 and 40847 discharges at their diagnostic times.

2.2. The core transport mixed B/gB model

The physical mechanism of the ITB formation has not yet been clearly identified. However, it is found that the suppression of core anomalous transport due to ω_{ExB} flow shear and magnetic shear causes ITB formations [10, 16]. ITB formation and its dynamics are modelled through a semi-empirical core transport model called mixed Bohm/gyro-Bohm (Mixed B/gB) [16]. It was originally a local transport model with Bohm scaling which means the diffusivities are proportional to the gyro-radius times the thermal velocity. These transport diffusivities are also functions of plasma parameters such as magnetic *q* and profile shapes. So in the simulations, all parameters are fixed while the gyro-radius is changed according to plasma dimensions. The Bohm model was initially derived for electron transport in JET tokamak [17]. Then, it was modified to additionally describe ion transport [18] and a new term called gyro-Bohm was added, in order to simulate results from both smaller and larger size tokamaks [19]. Gyro-Bohm scaling essentially means the diffusivities are proportional to the square of the gyro-radius times the thermal velocity divided by the plasma major radius. Usually, the Bohm term dominates over most of the plasma. The gyro-Bohm term contributes mainly in the deep core of the plasma and in small tokamaks with low heating power and low magnetic field. The Mixed B/gB transport model includes the ITB effect by having a cut-off in the Bohm term which is a function of flow shear and magnetic shear. The model can be expressed as the following:

$$\chi_e = 1.0\chi_{gB} + 2.0\chi_B, \qquad (2)$$

$$\chi_i = 0.5\chi_{gB} + 4.0\chi_B, \qquad (3)$$

$$D_H = D_Z = (0.3 + 0.7\rho)\frac{\chi_e \chi_i}{\chi_e + \chi_i}, \qquad (4)$$

where

$$\chi_{gB} = 5\times10^{-6}\sqrt{T_e}\left|\frac{\nabla T_e}{B_T^2}\right|, \qquad (5)$$

$$\chi_B = \chi_{B_0} \times \Theta\left(-0.14 + s - \frac{1.47\omega_{E\times B}}{\gamma_{ITG}}\right), \qquad (6)$$

With

$$\chi_{B_0} = 4\text{x}10^{-5} R\left|\frac{\nabla(n_e T_e)}{n_e B_T}\right| q^2 \left(\frac{T_e(0.8\rho_{max}) - T_e(\rho_{max})}{T_e(\rho_{max})}\right), \qquad (7)$$

where χ_e is the electron diffusivity, χ_i is the ion diffusivity, χ_{gB} is the gyro-Bohm contribution, χ_B is the Bohm contribution, D_H is the particle diffusivity, D_Z is the impurity diffusivity, ρ is normalized minor radius, T_e is the local electron temperature in keV, B_T is the toroidal magnetic field, s is the magnetic shear, ω_{ExB} is the shearing rate, γ_{ITG} is the linear growth rate, R is the major radius, and n_e is the local electron density. The linear growth rate γ_{ITG} can be calculated as v_{th}/qR, where v_{th} is the electron thermal velocity. The original Mixed B/gB model does not include the impurity transport. For simplicity, it is assumed in this work that the impurity transport is the same with the particle transport.

In this work, the ω_{ExB} shearing rate is calculated according to Hahm-Burrell model [20],

$$\omega_{ExB} = \left|\frac{RB_\theta^2}{B_T}\frac{\partial\left(E_r/RB_\theta\right)}{\partial\psi}\right|, \qquad (8)$$

where $B\theta$ is the poloidal magnetic field, Ψ is the poloidal flux, and E_r is the radial electric field, which can be calculated as follows:

$$E_r = \frac{1}{Zen_i}\frac{\partial p_i}{\partial r} - v_\theta B_T + v_{tor}B_\theta \qquad (9)$$

where $\frac{\partial p_i}{\partial r}$ is the pressure gradient, v_θ and v_{tor} are the poloidal and toroidal velocities, respectively, n_i is the ion density, Z is the ion charge number and e is the elementary charge. The calculation of toroidal velocity is discussed extensively in section 2.1.

2.3. The boundary pedestal model

In this study, the boundary condition of the plasma is set to be at the top of the pedestal which is where the edge transport barrier (ETB) is observed. The pedestal region is located at the steep gradient right near the edge of the plasma. It is assumed that the pressure gradient ($\partial p/\partial r$) within this region is constant so the pedestal temperature (T_{ped}) in keV unit can be calculated as follows [11]:

$$T_{ped} = \frac{1}{2kn_{ped}}\Delta\left|\frac{\partial p}{\partial r}\right| \qquad (10)$$

Where n_{ped} (m^{-3}) is pedestal density, k is the Boltzmann's constant, and Δ is the pedestal width. So in order to calculate pedestal temperature one must obtain pedestal density, pedestal width and pedestal gradient.

The pedestal pressure gradient scaling is limited by the ballooning mode instability [21]. It is based on the assumption that there exists a maximum normalized pressure gradient with critical pressure gradient, α_c,

$$\alpha_c(s,\delta,\kappa) = -\frac{2\mu_0 Rq^2}{{B_T}^2}\left(\frac{\partial p}{\partial r}\right)_c \qquad (11)$$

Here, κ is elongation, μ_0 is permeability of free space, R is the tokamak major radius, q is safety factor, and B_T is vacuum toroidal magnetic field. Rewrite this relation and substitute pressure gradient into equation (10) to obtain

$$T_{ped} = \frac{\Delta}{2kn_{ped}}\frac{\alpha_c {B_T}^2}{2\mu_0 Rq^2} \qquad (12)$$

The pedestal width scaling model is based on magnetic and flow shear stabilization ($\Delta \propto \rho_i s^2$) [11]. There is an assumption that the transport barrier is formed in the region where the turbulence growth rate is balanced by a stabilizing $E_r xB$ shearing rate. The scaling width is derived to be

$$\Delta = C_1 \rho s^2 = C_1\left(4.57x10^{-3}\frac{\sqrt{A_H T_{ped}}}{B_T}\right)s^2, \qquad (13)$$

where C_1 is the constant of proportionality and A_H is the average hydrogenic mass. Combine this scaling with previous pressure gradient scaling, the final T_{ped} is as follows

$$T_{ped} = C_1^{\,2}\left(\left(\frac{4.57x10^{-3}}{4\mu_0\left(1.6022x10^{-16}\right)}\right)^2\left(\frac{B_T^2}{q^4}\right)\left(\frac{A_H}{R^2}\right)\left(\frac{\alpha_c}{n_{ped}}\right)^2 s^4\right). \quad (14)$$

This result is used in BALDUR code to calculate the pedestal temperature which is the boundary condition for transport model and to eventually compute plasma profiles. The constant C_1 is chosen to minimize the RMSD with 533 experimental data points from four large tokamaks obtained from the ITPA pedestal database and from Ref. [11], it is found to be 2.42.

The pedestal density, n_{ped}, is obtained by an empirical model which is based on the fact that n_{ped} is a fraction of line average density, n_l, that can be taken from experimental data, as shown:

$$n_{ped} = 0.71 n_l \quad (15)$$

This pedestal density empirical model agrees with the data from the International Tokamak Physics Activity (ITPA) pedestal database with 12% RMSE [22].

3. Results and discussion

In this work, the simulations are carried out for ten JET optimized shear discharges [40542, 40847, 46123, 46664, 51599, 51976, 52009, 53521, 53532, and 53537] using BALDUR integrated predictive modeling code. These discharges are taken from the International Profile Database [23]. Table 1 summarizes the parameters for each discharge. These discharges are among the best results from JET with regards to the ITB formation that are available in the International Profile Database.

Table. 1 Summary of plasma parameters for 10 JET optimized shear discharges at the diagnostic time.

JET	Time (s)	R (m)	a (m)	I_p (MA)	B_T (T)	κ	δ	n_l (10^{19} m^{-3})
40542	47	2.93	0.94	3.22	3.49	1.64	0.35	2.41
40847	46	2.92	0.96	2.85	3.50	1.56	0.20	2.33
46123	46.5	2.89	0.98	2.50	2.54	1.52	0.17	2.24
46664	45.7	2.92	0.94	2.95	3.50	1.71	0.20	2.27
51599	46	2.89	0.96	2.21	2.64	1.66	0.23	1.90
51976	46.3	2.92	0.95	2.40	3.49	1.69	0.26	2.45
52009	21.6	3.01	0.88	2.49	2.70	1.72	0.47	7.30
53521	49	2.89	0.97	2.00	3.54	1.63	0.21	2.99
53532	46.5	2.89	0.96	2.22	2.64	1.67	0.23	2.52
53537	46.5	2.90	0.96	2.22	2.64	1.67	0.23	2.15

3.1 Comparisons of toroidal velocity profiles

To compare the toroidal velocity between simulation results of each model and experimental data, the diagnostic time of each JET discharge is chosen. The selection criteria are based on ITB and *H*-mode considerations. The profile plots of example discharges are shown in figure 2. Each demonstrates toroidal velocity as a function of normalized minor radius, the closed circles represent experimental data and the line represents simulation result of the model. It can be seen in discharges 46664 and 51599 the model over-predicts the experiments by up to factors of 5 and 3, respectively. Moreover, the general profile shape of the model is rather inconsistent especially near the edge of the plasma where the toroidal velocity values abruptly spike and then decrease to zero at the edge. This strange behavior is a result of numerical error due to how BALDUR computes the current density. BALDUR assumes that the current is zero at the edge, the value at the next grid spikes because BALDUR tries to conserve overall current flow.

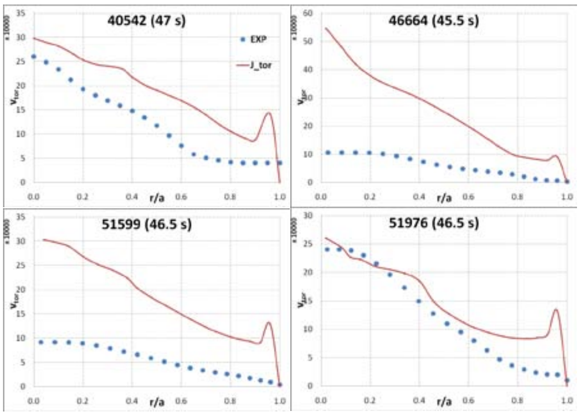

Fig. 2 Toroidal velocity profiles of selected JET discharges.

Quantitatively, the root mean square error (RMSE) comparisons and average offset values between simulation results and experimental data can be calculated by equations (16) and (17), respectively, as shown in table 2,

$$\mathrm{RMSE}(\%)=\sqrt{\frac{\sum_{i=1}^{N}\left(\ln\left(v_{tor\_\exp_i}\right)-\ln\left(v_{tor\_\mathrm{mod}_i}\right)\right)^2}{N-1}}\times 100, \quad (16)$$

$$\mathrm{Offset}=\frac{1}{N}\sum_{i=1}^{N}\left(\ln\left(v_{tor\_\exp_i}\right)-\ln\left(v_{tor\_\mathrm{mod}_i}\right)\right). \quad (17)$$

Table. 2 RMSE and its offset comparisons of toroidal velocity between experimental values and simulation results.

JET Discharge	***Results***	
	RMSE (%)	*Offset*
40542	26.33	-0.24
40847	88.84	-0.82
46123	64.86	-0.56
46664	200.46	-1.70
51599	146.04	-1.34
51976	16.99	-0.12
52009	25.61	-0.12
53521	21.94	-0.17
53532	45.12	-0.41
53537	94.00	-0.90
Average	73.02	-0.64

They confirm the qualitative observation described previously. The best agreement is found in discharge 51976 to be 16.99%. The negative sign in most of the offset values indicates that the model typically over-predict the experimental values. The average RMSE of the model is 73.02% with offset value of -0.64.

3.2 Comparison of plasma profiles

Figure 3 illustrates ion temperature time-evolution profiles of JET discharge 40542. The temperature gradient can be implied from the separation between each line which represents different position inside tokamak, ITB formation is the region of relatively wide separation. It can be concluded that when using experimental data of flow shear as an input, ITB formations can be successfully simulated for both position and time of the occurrences. However, when using experimental toroidal velocity as input only the occurrence's time is retained correctly, while ITB formations in the profile of theory-based model are relatively less pronounced. It is also worth noting that all simulations tend to under-predict the central ion temperature, but over-predict the pedestal temperature.

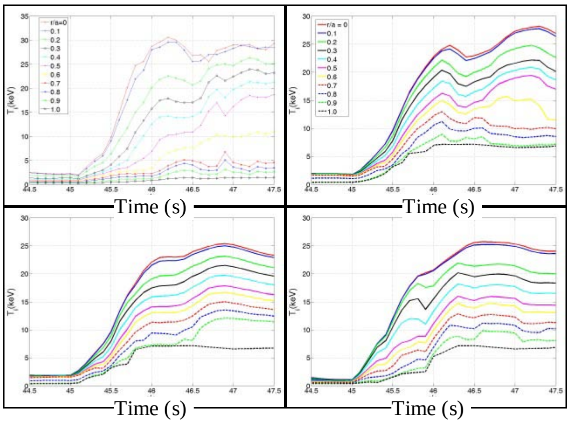

Fig. 3 JET 40542 Time-evolution profiles of T_i (keV): experimental data (top left) and simulation results using experimental ω_{ExB} (top right), experimental v_{tor} (bottom left), and the model (bottom right).

The plots illustrate the local ion temperature as a function of time with each line indicating a different position inside the plasma.

These lines are marked as normalized minor radius (*r/a*), where *r/a* = 0 represents plasma center, while *r/a* = 1 represents plasma edge. In the experiment, for example discharge 40542, the plasma was initiated with a fast current ramp, 0.5 MW of ICRH (ion cyclotron resonance heating) was applied for pre-heating. Later, NBI (neutral beam injection) power was stepped up from 0 to 10 MW at 45.0 seconds and then to 18 MW at 45.4 seconds. Experimentally, the ITB was formed at 45.4 seconds and persisted throughout the operation time.

To quantify the agreement of ion temperature, electron temperature, and electron density, the RMSE comparison between experimental data and simulation results of each JET discharge are calculated as follows:

$$\mathrm{RMSE}(\%) = \sqrt{\frac{1}{N}\sum_{i=1}^{N}\left(\frac{T_{\exp_i} - T_{\mathrm{mod}_i}}{T_{\exp_0}}\right)^2} \times 100 \text{ , } \quad (18)$$

$$\mathrm{Offset} = \frac{1}{N}\sum_{i=1}^{N}\left(\frac{T_{\exp_i} - T_{\mathrm{mod}_i}}{T_{\exp_0}}\right). \quad (19)$$

where *N* is total number of data, T_{expi} and T_{modi} are the i^{th} experimental and model results of temperature, and T_{exp0} is experimental temperature at the center of the tokamaks. In this experiment, there are a total of 5000 data points taken from International Pedestal Database for the statistical analysis. The electron temperature and density comparisons also use the similar calculation.

Fig.4 shows the RMSE deviations and offsets of ion temperature, electron temperature, and electron density, for each JET optimized shear discharges. These simulations are carried out by using predicted toroidal velocity model. It can be seen that the RMSE deviations vary from discharge to discharge, and from profile to profile, with a minimum of about 17% and a maximum of about 42% for the ion temperature profiles, with a minimum of about 15% and a maximum of about 64% for the electron temperature profiles, and with a minimum of about 12% and a maximum of about 21% for the electron density profiles.

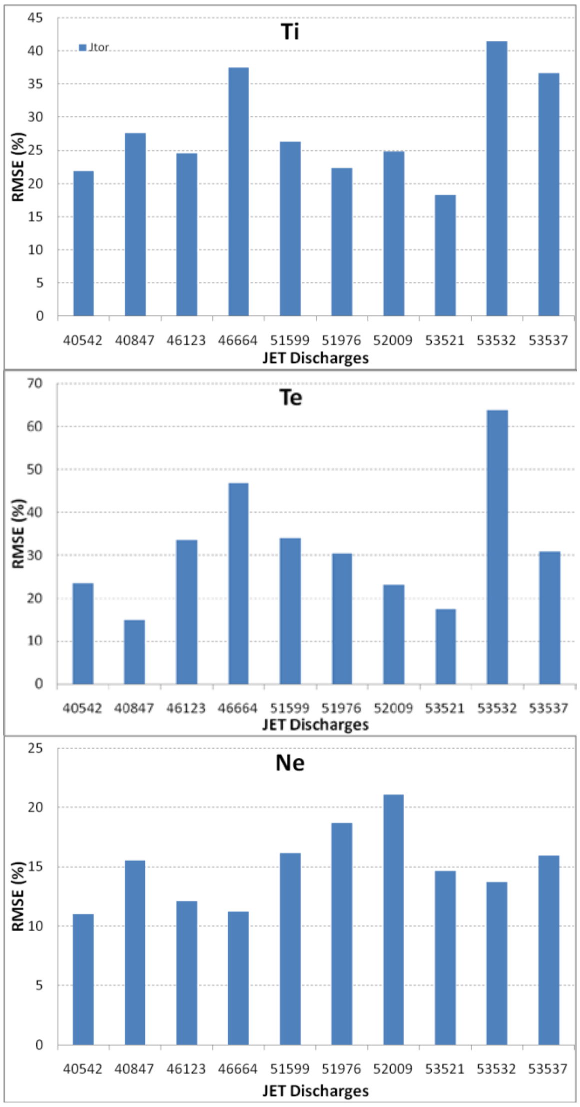

Fig. 4 RMSE comparison of each JET discharge for ion temperature (top), electron temperature (middle), and electron density (bottom).

4. Conclusion

A theoretical model for predicting toroidal velocity in ITB H-mode plasmas is developed and implemented in BALDUR integrated predictive modeling code, resulting in an improved predictive capability of the BALDUR code. The toroidal velocity is used by transport code in BALDUR to calculate the shearing rate which is believed to be the cause of ITB formation. The core transport model used in this study is called Mixed B/gB, which includes the effects of ITBs. The boundary is set to be at the top of the pedestal near the edge of the plasma with the boundary condition set by the ETB pedestal model, which is based on magnetic and flow shear stabilization combining with ballooning-mode limit instability. It is found that the toroidal velocity model resulted in a reasonable agreement between the predicted ion temperature and experimental results from 10 JET optimized shear discharges. The model can also successfully simulates formations of ITB inside the plasma.

5. Acknowledgement

This work is supported by the Commission on Higher Education (CHE) and the Thailand Research Fund (TRF) under Contract No RMU5180017. B. Chatthong thanks the Royal Thai Scholarship for educational support.

6. References

[1] Aymar, R., Barabaschi, P., and Shimomura, Y. (2002). The ITER design, *Plasma Phys. Control. Fusion*, vol. 44 (5), pp. 519.

[2] Hubbard, A.E. (2000). Physics and scaling of the H-mode pedestal, *Plasma Phys. Control. Fusion*, vol. 42 (5A), pp. A15.

[3] Connor, J.W., Fukuda, T., Garbet, X. *et al.* (2004). A review of internal transport barrier physics for steady-state operation of tokamaks, *Nucl. Fusion*, vol. 44 (4), pp. R1.

[4] Burrell, K.H. (1997). Effects of ExB velocity shear and magnetic shear on turbulence and transport in magnetic confinement devices, *Phys. Plasmas*, vol. 4 (5), pp. 1499-1518.

[5] Tala, T., Crombé, K., Vries, P.C.d. *et al.* (2007). Toroidal and poloidal momentum transport studies in tokamaks, *Plasma Phys. Control. Fusion*, vol. 49 (12B), pp. B291.

[6] Rozhansky, V., Kaveeva, E., Voskoboynikov, S. *et al.* (2002). Modelling of electric fields in tokamak edge plasma and L-H transition, *Nucl. Fusion*, vol. 42 (9), pp. 1110.

[7] Rogister, A.L., Rice, J.E., Nicolai, A. *et al.* (2002). Theoretical interpretation of the toroidal rotation velocity observed in Alcator C-Mod Ohmic H-mode discharges, *Nucl. Fusion*, vol. 42 (9), pp. 1144.

[8] Eriksson, A., Nordman, H., Strand, P. *et al.* (2007). Predictive simulations of toroidal momentum transport at JET, *Plasma Phys. Control. Fusion*, vol. 49 (11), pp. 1931.

[9] Chatthong, B., Onjun, T., and Singhsomroje, W. (2010). Model for toroidal velocity in H-mode plasmas in the presence of internal transport barriers, *Nucl. Fusion*, vol. 50 (6), pp. 064009.

[10] Tala, T.J.J., Heikkinen, J.A., Parail, V.V. *et al.* (2001). ITB formation in terms of $\omega_{E\times B}$ flow shear and magnetic shear s on JET, *Plasma Phys. Control. Fusion*, vol. 43 (4), pp. 507.

[11] Onjun, T., Bateman, G., Kritz, A.H. *et al.* (2002). Models for the pedestal temperature at the edge of H-mode tokamak plasmas, *Phys. Plasmas*, vol. 9 (12), pp. 5018-5030.

[12] Singer, C.E., Post, D.E., Mikkelsen, D.R. *et al.* (1988). Baldur: A one-dimensional plasma transport code, *Comput. Phys. Commun.*, vol. 49 (2), pp. 275-398.

[13] Onjun, T., and Pianroj, Y. (2009). Simulations of ITER with combined effects of internal and edge transport barriers, *Nucl. Fusion*, vol. 49 (7), pp. 075003.

[14] Hannum, D., Bateman, G., Kinsey, J. *et al.* (2001). Comparison of high-mode predictive simulations using Mixed Bohm/gyro-Bohm and Multi-Mode (MMM95) transport models, *Phys. Plasmas*, vol. 8 (3), pp. 964-974.

[15] Onjun, T., Bateman, G., Kritz, A.H. *et al.* (2001). Comparison of low confinement mode transport simulations using the mixed Bohm/gyro-Bohm and the Multi-Mode-95 transport model, *Phys. Plasmas*, vol. 8 (3), pp. 975-985.

[16] Erba, M., Cherubini, A., Parail, V.V. *et al.* (1997). Development of a non-local model for tokamak heat transport in L-mode, H-mode and transient regimes, *Plasma Phys. Control. Fusion*, vol. 39 (2), pp. 261.

[17] Taroni, A., Erba, M., Springmann, E. *et al.* (1994). Global and local energy confinement properties of simple transport coefficients of the Bohm type, *Plasma Phys. Control. Fusion*, vol. 36 (10), pp. 1629.

[18] Erba, M., Parail, V., Springmann, E. *et al.* (1995). Extension of a Bohm model for L-mode electron heat transport to ion heat transport and to the ohmic regime, *Plasma Phys. Control. Fusion*, vol. 37 (11), pp. 1249.

[19] Erba, M., Aniel, T., Basiuk, V. *et al.* (1998). Validation of a new mixed Bohm/gyro-Bohm model for electron and ion heat transport against the ITER, Tore Supra and START database discharges, *Nucl. Fusion*, vol. 38 (7), pp. 1013.

[20] Zhu, P., Bateman, G., Kritz, A.H. *et al.* (2000). Predictive transport simulations of internal transport barriers using the Multi-Mode model, *Phys. Plasmas*, vol. 7 (7), pp. 2898-2908.

[21] Connor, J.W. (1998). A review of models for ELMs, *Plasma Phys. Control. Fusion*, vol. 40 (2), pp. 191.

[22] Bateman, G., Onjun, T., and Kritz, A.H. (2003). Integrated predictive modelling simulations of burning plasma experiment designs, *Plasma Phys. Control. Fusion*, vol. 45 (11), pp. 1939.

[23] Boucher, D., Connor, J.W., Houlberg, W.A. *et al.* (2000). The International Multi-Tokamak Profile Database, *Nucl. Fusion*, vol. 40 (12), pp. 1955.